Global J. Environ. Sci. Manage. 11(4): 1547-1566, Autumn 2025, Serial #44

Global Journal of Environmental Science and Management
(GJESM)

Homepage: https://www.gjesm.net/

Podcasts

CASE STUDY

Potential impact of urbanization on heavy metals accumulation in surface soils of rapidly urbanizing cities

A. Zandybay[1], A. Kydyrova[1], A. Karilkhan[2], S. Gulnur[1], A. Daribay[1], T. Mkilima[3,*]

[1] *Department of Management and Engineering in Environmental Protection Education, L. N. Gumilyov Eurasian National University, Astana, Kazakhstan*

[2] *Department of Technological Equipment, Engineering and Standardization, Abylkas Saginov Karaganda Technical University, Karagandy, Kazakhsta*

[3] *Department of Environmental Engineering and Management, The University of Dodoma, 41218 Iyumbu, Dodoma, Tanzania*

ARTICLE INFO

Article History:
Received 07 May 2025
Revised 09 August 2025
Accepted 15 September 2025

Keywords:
Ecological risk indices
Heavy metal contamination
Human health risk assessment
Source apportionment
Urban soil pollution

DOI: 10.22034/gjesm.2025.04.11

ABSTRACT

BACKGROUND AND OBJECTIVES: Rapid urbanization significantly alters soil quality by influencing its chemical properties and accelerating the accumulation of toxic metals. Moreover, despite the extensive studies on vehicular emissions and their impact on metals like lead, zinc, and copper, limited studies have comprehensively examined how various human activities interact to shape heavy metal contamination across different urban gradients. This study addresses this critical knowledge gap by integrating high-resolution spatial analysis, multivariate statistical modeling, and ecological risk assessment to unravel the combined effects of transportation density, construction intensity, and industrial expansion on soil contamination.

METHODS: Ninety geo-referenced topsoil samples were collected from residential, industrial, recreational, and roadside areas. Ten priority toxic metals, including cadmium, lead, chromium, copper, zinc, nickel, cobalt, manganese, arsenic, and mercury, were analyzed using high-resolution mass spectrometry. To assess concentration patterns and identify possible sources of pollution, spatial interpolation and multivariate statistical analyses were employed. Additionally, human health and ecological risk assessments were conducted to evaluate potential hazards associated with soil contamination.

FINDINGS: Concentrations of metals revealed notable spatial differences across diverse urban land-use classifications. High-resolution inductively coupled plasma mass spectrometry detected high lead concentrations reaching 375 milligrams per kilogram and zinc up to 492.7 milligrams per kilogram. Cadmium concentrations, although lower in absolute terms, peaked at 2.1 milligrams per kilogram but contributed disproportionately to ecological risks. Mercury concentrations were relatively low, peaking at 0.9 milligrams per kilogram, whereas chromium, copper, and nickel levels were recorded at 142.6, 160.3, and 89.5 milligrams per kilogram, respectively, suggesting possible contributions from multiple sources beyond just vehicle emissions. Principal component analysis explained 78.3 percent of total variability and revealed three dominant components, with the first (34.7 percent) strongly influenced by lead, zinc, and copper, confirming traffic-related inputs.

CONCLUSION: The study underscores the notable effect of fast-paced urban development on soil contamination and delivers crucial information regarding the spatial distribution, sources, and risks associated with toxic metals in urban soils. These findings are essential for guiding land-use planning, environmental management, and the development of targeted mitigation strategies in rapidly expanding cities.

This is an open access article under the CC BY license (http://creativecommons.org/licenses/by/4.0/).

NUMBER OF REFERENCES	NUMBER OF FIGURES	NUMBER OF TABLES
37	5	7

*Corresponding Author:
Email: *tmkilima@gmail.com*
Phone: +255744698789
ORCID: 0000-0003-1170-0494

Note: Discussion period for this manuscript open until Dec 1, 2025 on GJESM website at the "Show Article".

INTRODUCTION

Urban soil pollution, particularly by heavy metals, has become an increasingly critical concern in the context of rapid urbanization, industrialization, and transportation activities. As cities progress and expand, the requirement for infrastructure and advancement escalates, causing a surge in emissions of pollutants, particularly heavy metals (Manzueta *et al.*, 2024; Idroes *et al.*, 2024). These metals, such as cadmium (Cd), lead (Pb), chromium (Cr), copper (Cu), zinc (Zn), nickel (Ni), cobalt (Co), manganese (Mn), arsenic (As), and mercury (Hg), have widespread environmental and human health implications due to their persistence and bioaccumulation in the ecosystem (Ali *et al.*, 2019; Mitra *et al.*, 2022; Hawrami and Baset, 2024). The quick development of metropolitan zones is commonly associated with poor waste management practices and limited enforcement of regulations, which intensifies the buildup of heavy metals in urban soils. These soils, being sinks for pollutants, absorb and store harmful substances, posing long-term risks to human health, especially in densely populated areas (Phaenark *et al.*, 2024). For instance, in the study conducted by Rana *et al.* (2024) in Bangladesh, it was observed that street dust in industrial areas exhibited significantly elevated concentrations of heavy metals, such as Mn at 444.35 milligrams per kilogram (mg/kg), Zn at 299.25 mg/kg, Cr at 238.31 mg/kg, and Pb at 54.22 mg/kg. The pollution load index (PLI) has been recorded at 2.45, signifying elevated contamination levels. Health risk assessments revealed heightened non-carcinogenic risks for children and possible cancer risks due to Cr exposure via inhalation, with values ranging from 1.13×10^{-4} to 5.96×10^{-4}. This highlights the serious health consequences of heavy metal buildup in urban areas. Heavy metals are unique in that they do not degrade over time and persist in the environment, making them a long-term threat to both ecological systems and human populations (Das *et al.*, 2023). These metals are toxic at even low concentrations and can accumulate in the food chain, leading to adverse effects on plants, animals, and humans. In urban settings, heavy metals build up in the soil, where they may be taken up by plants, consumed by animals, or inhaled by humans (Perković *et al.*, 2022). Long-term exposure to these contaminants can lead to various health problems, including developmental issues in children, neurological disorders, and increased cancer risk (Jaishankar *et al.*, 2014). The persistence of heavy metals in the environment, combined with their ability to bioaccumulate, makes it crucial to assess and mitigate the risks they pose to both the environment and public health, especially in urban settings where pollution levels are often higher. Much of the research has been directed towards heavy metal pollution in industrialized cities; however, the rising urban sprawl in developing nations brings forth a unique set of challenges. In these rapidly expanding urban centers, regulatory infrastructure may not yet be fully developed, leaving many areas vulnerable to unchecked pollution (Peter and Yang, 2019). Often, these cities are deficient in the monitoring and enforcement frameworks required to manage the emission of heavy metals and various pollutants, which makes them especially vulnerable to environmental deterioration. The absence of robust environmental regulations means that contamination levels are often underreported, and the full extent of pollution is unknown. This creates a significant gap in knowledge, particularly in fast-growing cities where the risk of contamination is high. Understanding the distribution, sources, and impacts of heavy metal pollution in these cities is crucial for implementing effective policies and interventions that can protect both human health and the environment. Urban soils function as a sink for contaminants originating from multiple human activities sources, including vehicle exhaust, industrial effluents, atmospheric deposition, and construction activities (Yang *et al.*, 2011). These sources continuously release heavy metals into the environment, where they are deposited on the soil surface. The emissions produced by vehicles, especially those that are older and utilize fuels containing higher levels of metals, significantly contribute to the presence of metals like Pb, Zn, and Cu in urban soils (Kuklová *et al.*, 2022). Industrial activities, including the burning of fossil fuels, waste incineration, and manufacturing processes, are also major contributors. Furthermore, atmospheric deposition, where pollutants are transported by wind and settled on the ground, intensifies contamination levels (Amodio *et al.*, 2014). The combination of these diverse sources makes urban soils a key medium for monitoring environmental pollution. Comprehending the accumulation of pollutants in urban soils is vital for creating effective strategies to manage contamination and reduce its consequences

(Luo *et al.*, 2024). The topsoil layer of urban soils tends to accumulate pollutants more readily than deeper soil layers, making it a critical medium for monitoring environmental quality (Yang *et al.*, 2024). This is particularly true for heavy metals, which are often immobile in soil and remain concentrated in the upper layers. Given that the topsoil is the primary area for various human activities such as agriculture, construction, and recreation, it represents the most probable point of human interaction (Sánchez-Castro *et al.*, 2023). Through the identification of contamination patterns in urban soils, researchers can locate areas with significant exposure and evaluate the corresponding risks to both human health and ecosystems (Proshad *et al.*, 2024). This information is essential for guiding urban planning and policy decisions, such as zoning, land use, and public health interventions. Comprehending how pollutants are spatially distributed in urban soils enables focused actions that can minimize exposure, especially in sensitive locations like residential neighborhoods, schools, and playgrounds. Despite the swift expansion of cities around the globe increasing human-induced pressures on urban ecosystems, resulting in significant heavy metal pollution in soils, the overall scope, distribution, and ecological hazards of these contaminants—especially in developing urban areas—are still not well comprehended. Moreover, despite increasing concerns about urban soil contamination, previous studies in Central Asia and globally have largely focused on isolated sources, such as vehicular emissions or industrial discharges, without integrating multiple anthropogenic drivers or assessing their combined ecological risks across urban gradients. This study bridges that gap by providing the first comprehensive assessment that integrates high-resolution spatial analysis, multivariate statistical modeling, and ecological risk evaluation to examine how diverse urban activities collectively influence heavy metal contamination across residential, industrial, recreational, and roadside soils in Astana, Kazakhstan. The aim of this study was to evaluate the impact of rapid urbanization on heavy metal contamination in surface soils of Astana, Kazakhstan. It focuses on assessing the concentrations, spatial distribution, and potential sources of ten priority heavy metals. An integrated multi-method strategy was utilized, incorporating geostatistical analysis, receptor modeling, along with evaluations of human and ecological risks. This study addresses this critical gap by providing detailed spatial and risk-based insights into heavy metal contamination across diverse land-use zones with a case of Astana, Kazakhstan, conducted in 2024.

MATERIALS AND METHODS

Soil sampling and site selection

A total of 90 surface soil samples with depth: 0–20 centimeters (cm) were collected during the dry season to minimize moisture-related variability (Fig. 1). The study area was systematically stratified into four predominant urban land-use categories: residential (n = 25), industrial (n = 25), recreational (n = 20), and roadside (n = 20). Sampling sites were previously identified utilizing a randomized grid overlay method in a geographic information system (GIS) to guarantee representative coverage. At each site, three subsamples were collected within a 1-meter radius and homogenized to form one composite sample. All sampling points were geo-referenced using a handheld global positioning system (GPS) unit (Garmin GPSMAP 64s) with a positional accuracy of ±3 meters (m) to enable precise spatial analysis and geostatistical modeling. Baseline concentrations of metals in the soil were determined using surface samples (0–20 cm) collected from peri-urban regions of Astana that are minimally influenced by industrial, traffic, or other human activities. Reference sites were selected to match the soil texture, parent material, and geomorphology of the urban study locations. At each site, three subsamples within a 1-meter radius were homogenized to form a composite sample. The average concentrations derived from these reference soils were employed to determine local geochemical background values, which represent the natural features of the region.

Sample preparation and heavy metal analysis

The soil samples underwent air drying at ambient laboratory conditions, maintaining a temperature of 20 to 25 degrees Celsius (°C) for 72 hours. Subsequently, they were gently disaggregated and passed through a 2 millimeters (mm) polyethylene mesh to remove gravel and organic debris (Fig. 1). For metal analysis, 0.5 grams (g) of each dried soil sample was digested using aqua regia (hydrochloric acid (HCl): nitric acid (HNO_3) = 3:1 volume-to-volume ratio) following the United States Environmental Protection



(a) (b)

Fig. 1: Soil sampling at different locations (a) roadside (b) recreational

Agency (USEPA) Method 3051A (Bettinelli *et al.*, 2000) in a microwave-assisted digestion system (CEM Mars 6, USA). The digests were filtered, diluted to 50 milliliters (mL) with ultrapure water with resistivity >18.2 megaohm-centimeter (MΩ·cm), and analyzed using inductively coupled plasma mass spectrometry (ICP-MS, Agilent 7900). The target elements included Cd, Pb, Cr, Cu, Zn, Ni, Co, Mn, As, and Hg. In order to maintain data quality and reliability, each analytical batch included certified reference materials (NIST SRM 2711a), method blanks, and duplicate samples. Recovery rates ranged from 91 percent (%) to 106%, and relative standard deviations (RSDs) for replicate analyses were maintained below 5%. Soil samples were analyzed for key physicochemical properties known to influence metal mobility, including pH, organic matter (OM), and cation exchange capacity (CEC). Soil pH was measured in a 1:2.5 soil-to-water suspension using a calibrated pH meter, revealing a slightly alkaline to neutral range (7.2–7.8), which can reduce the solubility of many metals such as Pb and Cu. Using the Walkley–Black method, the organic matter content was assessed to be between 2.1% and 3.8%, which reflects a moderate potential for complexation capable of immobilizing metals including Cd and Zn. CEC, measured by the ammonium acetate technique, fluctuated between 12–24 cmol/kg, reflecting the soil's ability to hold cations and regulate metal availability. These parameters collectively offer insight into metal mobility and bioavailability in Astana's urban soils.

Spatial distribution and geostatistical analysis

The spatial variability of heavy metal concentrations was analyzed using ArcGIS Pro 3.2 (ESRI, USA). Ordinary kriging, a robust geostatistical interpolation method, was applied to develop spatial distribution maps for each metal. Data normality was assessed prior to interpolation and improved using log transformation as needed. Semivariograms were modeled and cross-validated using root mean square error (RMSE) and mean standardized error metrics. To evaluate the presence of spatial autocorrelation, the Global Moran's I statistic was computed, revealing whether the distribution patterns of heavy metals were clustered, dispersed, or random. Moran's I and semivariogram analysis were employed to test the spatial autocorrelation of metal concentrations, assessing the level of clustering or dispersion in the study area. Significant positive Moran's I values ($p < 0.05$) confirmed that metal concentrations were not randomly distributed but exhibited spatial dependence, justifying the use of geostatistical interpolation methods such as ordinary

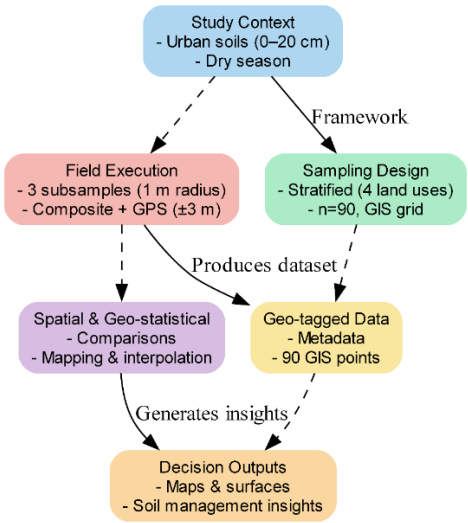

Fig. 2: Soil sampling conceptual framework

kriging. An exponential model was employed to fit semivariogram models, optimizing nugget, sill, and range parameters for each metal, followed by cross-validation to determine prediction accuracy. High correlation coefficients ($r^2 > 0.85$) and low root mean square errors (RMSE) indicated robust interpolation, supporting reliable spatial mapping of contamination hotspots and informing targeted risk management.

Multivariate statistical analysis

Potential contamination sources and underlying data structures were identified using principal component analysis (PCA) with varimax rotation and hierarchical cluster analysis (HCA) based on Ward's method with squared Euclidean distance. The suitability of the data for PCA was verified using the Kaiser-Meyer-Olkin (KMO) test and Bartlett's test of sphericity. To quantify the contribution of potential pollution sources, positive matrix factorization (PMF 5.0), developed by the US EPA, was employed. The model underwent various iterations with different factor counts, and the most interpretable solution was selected based on minimized Q values and residuals. The calculation of uncertainty inputs was based on both instrumental errors and the detection limits of the method. Fig. 2 presents the conceptual framework of the study, outlining the progression from study context and sampling design through field execution and data generation to spatial analysis and decision-oriented outputs.

Human health risk assessment

The human health risk was assessed for two sensitive population groups; children (1–6 years) and adults (30–60 years); following US EPA guidelines of risk assessment guidance for superfund (RAGS), Part A). Exposure pathways included ingestion, inhalation of soil particles, and dermal contact. For each pathway, the average daily intake (ADI) was calculated by utilizing standard equations that account for exposure frequency, duration, and body weight. Non-carcinogenic risk assessment was conducted through the hazard quotient (HQ) and hazard index (HI), whereas the evaluation of carcinogenic risk (CR) relied on element-specific cancer slope factors (CSFs). An HI >1 indicates potential for adverse health effects, while a CR range of 10^{-6} to 10^{-4} was considered acceptable.

Ecological risk assessment

Two complementary indices were utilized to fully evaluate the ecological risks related to heavy metal contamination in urban soils. The first index, the potential ecological risk index (PERI), integrates three key parameters: the measured concentration of each metal, its respective toxicity response coefficient, and the natural background concentration. Initially, the ecological risk factor for each element is identified, and subsequently, the cumulative risk for all metals is calculated to produce the overall PERI value. This approach enables the classification of ecological risk

levels as low, moderate, considerable, or very high. In this study, Cd and Hg were the most significant contributors to ecological risk, particularly in industrial and roadside zones, with individual risk factors (Er_i) exceeding 160 and 120, respectively. These values identified the areas as experiencing significant to high ecological risk, highlighting the impact of industrial discharge and vehicular emissions. The PERI framework proved effective in identifying pollutant-specific threats and in prioritizing zones requiring urgent ecological management, using Eqs. 1 and 2 (Chen *et al.*, 2019; Custodio *et al.*, 2021):

$$Er_i = T_i \times \left(\frac{C_i}{B_i} \right) \quad (1)$$

$$PERI = \sum Er_i \quad (2)$$

Where, Er_i = Ecological risk factor for the individual metal i, T_i = Toxic response factor for metal i (e.g., Cd = 30, Hg = 40, As = 10, etc.), C_i = Measured concentration of metal i in the soil (mg/kg), B_i = Background concentration of metal i in the soil (mg/kg), usually derived from regional geochemical baselines.

Two complementary indices were adopted to fully evaluate the ecological risks tied to heavy metal contamination in urban soils. The primary index, referred to as the PERI, incorporates three vital parameters: the concentration of each metal that has been measured, its associated toxicity response coefficient, and the natural background concentration. The ecological risk factor for each element is first determined, and then the cumulative risk across all metals is computed to yield the overall PERI value. This approach enables the classification of ecological risk levels as low, moderate, considerable, or very high. In this study, Cd and Hg were the most significant contributors to ecological risk, particularly in industrial and roadside zones, with Er_i exceeding 160 and 120, respectively. These values designated the zones as facing significant to high ecological risk, underscoring the impact of industrial discharge and vehicular emissions. The PERI framework proved effective in identifying pollutant-specific threats and in prioritizing zones requiring urgent ecological management, using Eq. 3 (Custodio *et al.*, 2021):

$$I_{geo} = log_2 \left(\frac{C_n}{1.5 \times B_n} \right) \quad (3)$$

Where, Igeo = Geoaccumulation index for a given heavy metal, C_n = measured concentration of the metal in the soil (mg/kg), B_n = Geochemical background concentration of the same metal (mg/kg), 1.5 = Constant factor that accounts for potential variations in background data due to lithogenic (natural) variability, log_2 = Base-2 logarithm used to scale the index.

Soil microbial activity assessment

In order to better comprehend the ecological consequences of heavy metal contamination, soil microbial activity was analyzed in a group of 36 representative samples collected from residential, industrial, recreational, and roadside areas. Microbial biomass carbon (MBC) was determined using the chloroform fumigation–extraction method, while basal soil respiration (BSR) was measured through carbon dioxide (CO_2) evolution over a 7-day incubation period at 25 ± 1 °C. Furthermore, the quantification of dehydrogenase enzyme activity (DHA) was conducted colorimetrically through the reduction of triphenyltetrazolium chloride (TTC), since DHA is a sensitive indicator of microbial metabolic potential. These microbial endpoints were selected because they provide early signals of ecosystem stress caused by heavy metal contamination. To ensure quality control, measurements were conducted in triplicate, and all microbial parameters were standardized to the dry weight of the soil for comparative analysis among various land-use types.

RESULTS AND DISCUSSION

The background soil concentrations in peri-urban areas of Astana indicate generally low levels of metals, reflecting minimal anthropogenic influence and natural geochemical conditions. Pb, Zn, Cu, and Ni show slightly higher values compared to other metals but remain well below urban contamination thresholds, consistent with natural mineralization in the region. Cd, As, and Hg demonstrate extremely low levels, indicating minimal contribution from industrial, vehicular, or agricultural activities. Mn and Cr are relatively higher but display low variability, characteristic of the local soil parent material (Fig. 3).

Descriptive statistics of heavy metal concentrations

The concentrations of heavy metals in the urban soils of Astana reveal both notable similarities and

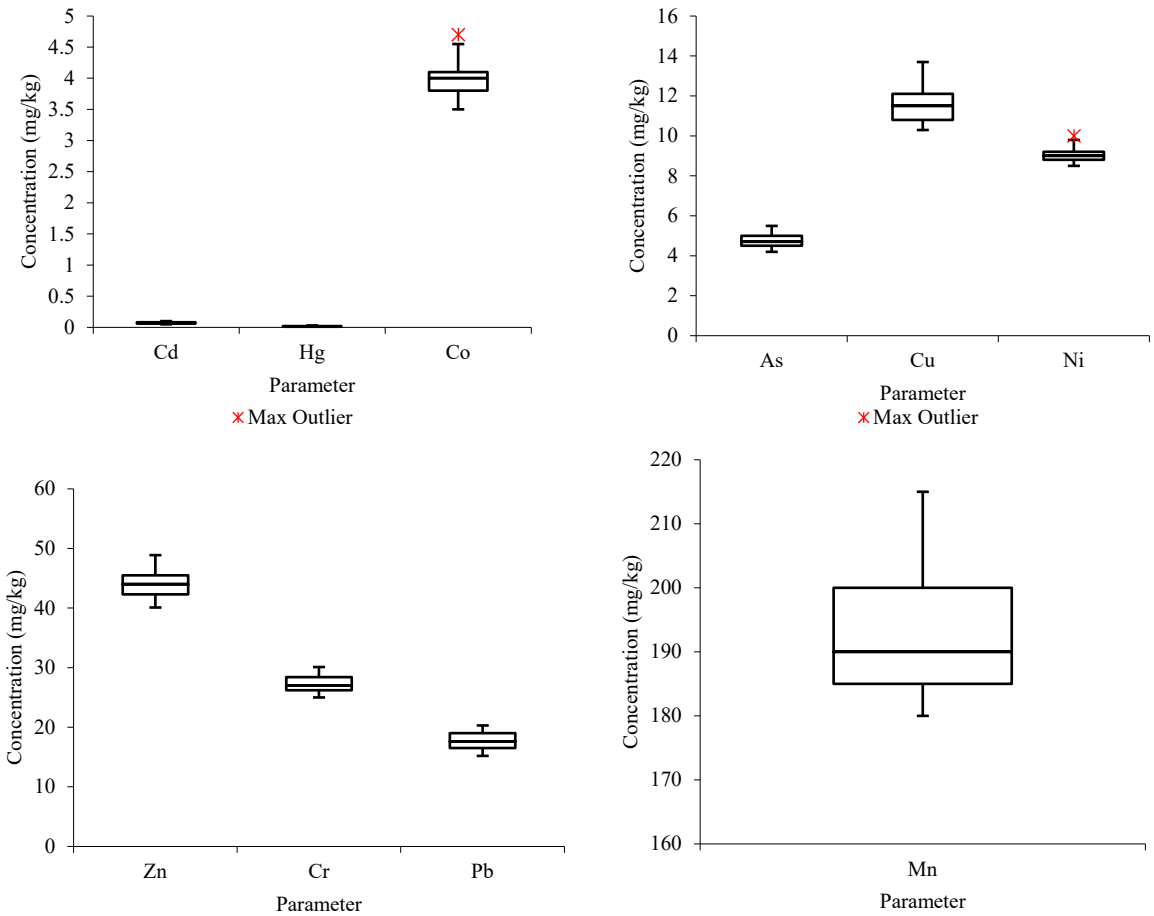

Fig. 3: Boxplots showing the distribution of baseline soil metal concentrations

differences in comparison to other fast-developing cities with comparable climatic conditions and development trajectories. The elevated concentrations of Pb, Cd, and Hg observed in Astana, with maximum values reaching 375 mg/kg, 2.1 mg/kg, and 0.9 mg/kg, respectively, exceed international soil quality guidelines and indicate strong anthropogenic influence, particularly near roadside and industrial zones. This pattern is consistent with studies from Wuhan, China, where accelerated industrialization and congested transportation networks have led to pronounced spatial heterogeneity of Pb and Cd. The use of geographically weighted regression (GWR) models has uncovered strong links between heavy metal hotspots and anthropogenic drivers (Sun *et al.*, 2025). However, unlike Wuhan, where Cu and cadmium concentrations are more influenced by natural geochemical backgrounds, Astana exhibits consistently elevated Cu levels (mean 74.5 mg/kg) and significant cadmium variability (%CV 67.1%), pointing toward localized contamination from industrial emissions, electronic waste disposal, and traffic-derived particulates. Comparisons with Nanchang, China, further underscore Astana's distinctive contamination profile. In Nanchang, soil Pb, Cd, and Cr levels decrease markedly with increasing urbanization intensity due to enhanced sequestration by glomalin-related soil proteins (GRSP), which exhibit strong adsorption capacities for heavy metals (Tu *et al.*, 2025). Conversely, the consistently elevated levels of Pb and Cd in Astana, even in newer urban districts, indicate a lack of effective natural attenuation mechanisms. This likely reflects lower organic matter content and diminished GRSP-mediated

sequestration under semi-arid climatic conditions. Similarly, findings from Łódź, Poland, a post-industrial city with a comparable continental climate, reveal high Zn, Pb, and Cu enrichment near industrial and high-traffic zones, where approximately one-third of urban soils are highly contaminated (Wieczorek *et al.*, 2020). Yet, Astana shows broader spatial variability, with coefficients of variation exceeding 60% for several metals, reflecting both localized hotspots and a less uniform distribution compared to Łódź's more spatially clustered contamination (Table 1).

Spatial distribution and hotspot identification

Table 2 presents the spatial distribution and clustering of heavy metals across the urban landscape, complementing the raw concentrations reported in Table 1. The analysis identified specific patterns that are significantly connected to land use, notably regarding transportation and industrial activities. Kriging interpolation maps identified clear hotspots of Pb, zinc, and copper along major transportation corridors. These metals, connected to vehicle exhaust, tire degradation, brake components, and road abrasion, displayed higher levels in traffic zones, affirming that vehicular emissions as a major contributor. Pb (38–276 mg/kg) and Cu (36–151 mg/kg) showed localized contamination, while high Moran's I values (e.g., 0.64 for copper) indicated strong clustering, suggesting that mitigation should focus on densely populated corridors. Industrial zones displayed a contrasting pattern dominated by Cr, Ni and Co. Maximum concentrations reached 87 mg/kg for Cr, 62 mg/kg for Ni, and 49 mg/kg for Co, mainly around manufacturing plants and metal workshops. Moran's I values for Cr (0.55), Ni (0.57), and Co (0.60) confirmed significant spatial clustering, reflecting industrial emissions, runoff, and atmospheric deposition. Ongoing pollution in these regions necessitates focused actions like enhanced emission regulations and site-specific cleanup efforts. In contrast, Hg and As showed broader, more diffuse distributions. Concentrations were lower (0.02–0.76 mg/kg for Hg, 0.04–0.68 mg/kg for As) but extended citywide, likely influenced by long-range atmospheric deposition. Lower Moran's I values (0.48 for Hg, 0.43 for As) indicate dispersed patterns, emphasizing the need for citywide policies and emission controls.

Correlation analysis

The Pearson correlation analysis provided insights

Table 1: Descriptive statistics of heavy metal concentrations in urban soil samples (mg/kg)

Metal	Minimum	Maximum	Mean	Standard deviation (SD)	%CV
Cd	0.08	2.1	0.76	0.51	67.1
Pb	12.5	375	112.3	76.8	68.4
Cr	18.4	142.6	63.7	28.1	44.1
Cu	15.1	160.3	74.5	35.4	47.5
Zn	27.6	492.7	158.9	91.2	57.4
Ni	7.4	89.5	32.1	19.7	61.4
Co	4.3	36.2	18.5	8.2	44.3
Mn	174	693.5	331.6	102.9	31
As	1.2	35.7	14.6	7.3	50
Hg	0.03	0.9	0.31	0.18	58.1

Table 2: Summary of spatial distribution of heavy metals and hotspot identification

Metal	Zone of highest concentration	Concentration range (mg/kg)	Spatial pattern	Global Moran's I Value ($p < 0.01$)
Pb	Major transportation corridors	38 - 276	Clustered, hotspot near traffic zones	0.62
Zn	Major transportation corridors	47 - 158	Clustered, with high concentrations in traffic zones	0.59
Cu	Major transportation corridors	36 - 151	Clustered, hotspots near roads	0.64
Cr	Industrial zones	22 - 87	Concentrated near industrial areas	0.55
Ni	Industrial zones	14 - 62	Clustered near industrial sites	0.57
Co	Industrial zones	9-49	High in industrial zones	0.6
Hg	Diffuse distribution, city-wide	0.02 - 0.76	Diffuse, atmospheric deposition	0.48
As	Diffuse distribution, city-wide	0.04 - 0.68	Diffuse, atmospheric deposition	0.43

into potential sources and interrelationships among heavy metals in urban soils. Strong positive correlations were observed between Pb and Zn (r = 0.84), Cu and Zn (r = 0.79), and Cr and Ni (r = 0.82), suggesting common anthropogenic origins. These metals are generally associated with traffic emissions, wear from tires and brakes, industrial discharges and urban runoff. The strong Pb-Zn and Cu-Zn correlations likely reflect combined deposition from vehicular activity, while the Cr-Ni association points toward industrial operations, such as metal processing and electroplating, as major contributors. These patterns confirm trends in spatial distribution and underscore the necessity of focusing on particular pollution sources. Moderate correlations were observed between Hg and As (r = 0.56), indicating partially shared contamination sources. Given the diffuse spatial patterns of these elements, atmospheric deposition from fossil fuel combustion, small-scale industrial emissions, or legacy pesticide applications is a likely pathway. This moderate correlation implies that dispersion occurs at a regional level rather than from specific localized sources. Despite weaker association, Hg and As remain environmentally significant due to their toxicity and persistence. In contrast, Mn and Co exhibited weak or non-significant correlations with most metals; Mn had a maximum correlation of r = 0.33 with Co. This implies that Mn and Co primarily originate from geogenic or naturally occurring sources rather than anthropogenic activities. Mn reflects underlying soil geology, while Co variability is less influenced by shared contamination pathways compared to other metals. The correlation matrix (Table 3) complements spatial and statistical assessments, clustering metals into strong, moderate, and weakly associated groups. These classifications can facilitate the identification of pollution sources, spotting co-existing contaminants, and creating effective monitoring strategies. For example, Zn monitoring may provide indirect information on Pb and Cu due to their high interdependence, reducing analytical workload. On the contrary, metals that exhibit low correlation, like Mn and Co, point to the importance of management strategies that are centered on geological evaluations.

Principal component analysis

The PCA carried out in this study is a strong statistical tool designed to uncover the intricate sources of heavy metal pollution in urban soils. The analysis revealed three major principal components (PCs) that collectively explained 78.3% of the total variance in the dataset, indicating a high degree of structure and interpretability. PC1 alone accounted for 34.7% of the variance and was strongly influenced by Pb, Zn, and Cu, all of which are well-established tracers of vehicular emissions. Their high loading values; Pb (0.87), Zn (0.82), and Cu (0.79); reflect a shared origin, most likely from vehicle exhaust, brake pad wear, and tire degradation. This component corresponds with previous spatial analyses that recognized major roadways and transportation corridors as critical hotspots for these metals, implying that vehicular activity is a major factor in urban soil contamination. PC2 explained 27.1% of the total variance and exhibited high loadings for Cr, Ni, and Co, which are typically associated with industrial processes. Cr (0.85), Ni (0.83), and Co (0.76) all demonstrated strong interrelationships, suggesting emissions from similar anthropogenic activities such as metal processing, alloy manufacturing, and electroplating industries. The spatial distribution data reinforces these findings, revealing increased levels of these metals near industrial regions. This principal component underscores the localized but intense impact of industrial operations on soil contamination and points to the necessity of implementing stricter emission controls in such

Table 3: Pearson correlation coefficients between heavy metal concentrations in urban soils (n = 90).

Metal	Cd	Pb	Cr	Cu	Zn	Ni	Co	Mn
Cd	1	0.63	0.55	0.6	0.66	0.51	0.32	0.25
Pb	0.63	1	0.44	0.68	0.84	0.39	0.29	0.22
Cr	0.55	0.44	1	0.56	0.59	0.82	0.46	0.28
Cu	0.6	0.68	0.56	1	0.79	0.43	0.3	0.19
Zn	0.66	0.84	0.59	0.79	1	0.47	0.35	0.23
Ni	0.51	0.39	0.82	0.43	0.47	1	0.38	0.26
Co	0.32	0.29	0.46	0.3	0.35	0.38	1	0.33
Mn	0.25	0.22	0.28	0.19	0.23	0.26	0.33	1

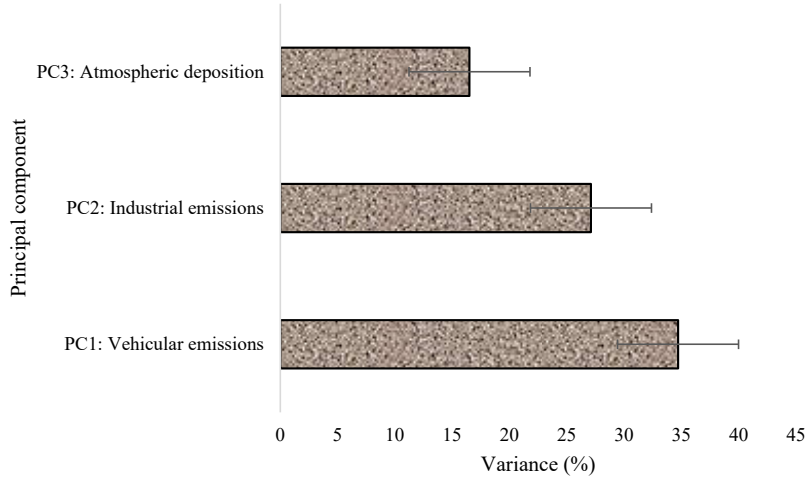

Fig. 4: PCA for heavy metal concentrations

areas. Furthermore, the presence of these metals in substantial amounts heightens concerns about both occupational and residential exposure for those living in proximity to industrial facilities. The third principal component (PC3), accounting for 16.5% of the variance, was primarily influenced by Hg and As, with exceptionally high loadings of 0.91 and 0.89, respectively. These components are usually released into the environment via atmospheric deposition caused by coal burning, pesticide application, and the long-distance movement of airborne pollutants. Unlike the localized patterns observed for vehicular and industrial metals, Hg and As were more diffusely distributed throughout the study area, as revealed in the spatial analysis. This widespread distribution suggests contributions from regional or even global sources and highlights the insidious nature of airborne pollutants. The close relationship between Hg and As in this component indicates a wider environmental concern, since both metals are harmful even in minimal amounts are likely to remain in the environment, presenting enduring threats to human health and ecological stability (Fig. 4).

The PCA results provide a comprehensive framework for interpreting the contamination profile of urban soils. Through the identification of specific elements related to vehicular, industrial, and atmospheric sources, the analysis provides a clearer insight into the sources of pollution and possible exposure routes. The clear separation of metals into these three categories reinforces previous findings from correlation and spatial analyses, lending robustness to the overall interpretation. Importantly, these insights are crucial for guiding environmental management strategies and policy interventions. As an illustration, pollution from traffic can be alleviated by using green buffers and regulating vehicle emissions, whereas industrial emissions call for focused remediation and tighter compliance standards. Addressing atmospheric deposition, however, may demand broader regional or international cooperation. Collectively, the PCA underscores the multifaceted nature of urban soil contamination and the need for integrated monitoring and control strategies (Table 4).

Source apportionment via positive matrix factorization (PMF)

The PMF model decomposed the heavy metal dataset into three distinct source profiles, consistent with PCA results. Traffic-related emissions (Factor 1) were the dominant contributor, accounting for 46% of the total metal burden, with Pb, Zn, and Cu as primary indicators. These metals are strongly associated with vehicle-related activities, including fuel combustion, brake wear, tire degradation, and engine oil leakage, consistent with observed hotspots identified near heavily trafficked areas. Industrial discharges (Factor 2) contributed 32% of the contamination load, characterized by high levels of Cr, Ni, and Co, commonly associated with metal finishing, electroplating, and

Table 4: Results of PCA for heavy metal concentrations

Principal Component	Heavy metal loadings
PC1: Vehicular emissions	Pb (0.87), Zn (0.82), Cu (0.79)
PC2: Industrial emissions	Cr (0.85), Ni (0.83), Co (0.76)
PC3: Atmospheric deposition	Hg (0.91), As (0.89)

Table 5: Source apportionment results from PMF for heavy metal concentrations in urban soils

Source	Factor	Contribution (%)	Dominant metals	Correlation (Observed vs. Reconstructed)
Traffic-related emissions	Factor 1	46%	Pb, Zn, Cu	r > 0.85
Industrial discharges	Factor 2	32%	Cr, Ni, Co	r > 0.85
Atmospheric deposition	Factor 3	22%	Hg, As	r > 0.85

alloy manufacturing. Their presence in industrial areas, along with the robust agreement found in PCA and spatial hotspot mapping, underscores the site-specific consequences of industrial activities and the urgent requirement for tighter emission regulations. Atmospheric deposition (Factor 3) accounted for the remaining 22%, dominated by Hg and As, which are introduced through fossil fuel combustion, pesticide use, and long-range transport of airborne pollutants. In contrast to the other elements, this source showed a diffuse spatial distribution, reflecting the effects of regional and transboundary contributions that are more difficult to control locally. Model validation showed strong correlations ($r > 0.85$) between observed and reconstructed concentrations, confirming the robustness of the PMF results. The integration of PMF, PCA, and spatial analysis provides a comprehensive understanding of heavy metal origins in urban soils. These quantified contributions provide support for evidence-based interventions, such as targeted traffic emission controls, more stringent industrial regulations, and regional air quality management strategies aimed at effectively reducing contamination (Table 5).

Human health risk assessment

The assessment of human health risks indicated significant disparities in vulnerability levels between children and adults, underscoring the heightened exposure risks that children experience as a result of their greater soil ingestion rates and enhanced physiological sensitivity. In the evaluated urban zones, hazard index (HI) values for children frequently exceeded the critical threshold of 1, particularly for Pb and As, indicating significant potential for non-carcinogenic effects. The highest risks were observed in industrial zones, where HI values reached 1.48 for Pb and 1.21 for As, while roadside areas also showed elevated risks. When assessed against international soil quality benchmarks, these metrics highlight substantial issues. As an illustration, the maximum permissible concentration (MPC) for lead (Pb) in Kazakhstan is set at 32 mg/kg, but the soil concentrations in high-exposure regions have been found to exceed this limit by up to 4.8 times. Similarly, As levels surpassed recommended thresholds outlined by the U.S. Environmental Protection Agency (0.5 mg/kg for residential soils) and Canadian guidelines (12 mg/kg), underscoring that children in industrial and roadside areas are exposed to metal concentrations well above safe limits. Comparable benchmarks from Europe, including Denmark (Pb: 40 mg/kg, As: 0.3 mg/kg) and the Netherlands (Pb: 85 mg/kg, As: 0.8 mg/kg), further reinforce the severity of these exceedances. The outcomes underscore the pressing requirement for focused mitigation actions, which include soil remediation, restricting children's access to polluted sites, and promoting community health education initiatives. For adults, HI values across all urban zones remained below the critical threshold of 1, suggesting a minimal likelihood of non-carcinogenic effects under current exposure scenarios. Nevertheless, moderately elevated HI values for Pb (0.73) and As (0.70) in industrial and roadside zones suggest that chronic or occupational exposure could still pose long-term health risks, particularly for sensitive populations such as pregnant individuals. In conjunction with non-carcinogenic risks, the carcinogenic risks related to As exposure were analyzed. Industrial and roadside areas exhibited

Table 6: Human health risk assessment for heavy metal contamination in urban soils, disaggregated by exposure pathway and population group

Zone	Metal	Exposure pathway	Child HI	Adult HI	Carcinogenic risk (CR): As
Industrial Zone	Pb	Ingestion	0.82	0.42	–
		Inhalation	0.31	0.18	–
		Dermal Contact	0.35	0.13	–
		Total (HI)	1.48	0.73	–
	As	Ingestion	0.7	0.31	1.3×10^{-4}
		Inhalation	0.25	0.12	1.3×10^{-4}
		Dermal Contact	0.26	0.11	1.3×10^{-4}
		Total (HI)	1.21	0.54	1.3×10^{-4}
Roadside Zone	Pb	Ingestion	0.77	0.39	–
		Inhalation	0.29	0.17	–
		Dermal Contact	0.32	0.14	–
		Total (HI)	1.38	0.7	–
	As	Ingestion	0.68	0.3	1.2×10^{-4}
		Inhalation	0.25	0.11	1.2×10^{-4}
		Dermal Contact	0.26	0.11	1.2×10^{-4}
		Total (HI)	1.19	0.52	1.2×10^{-4}
Recreational Zone	Pb	Ingestion	0.52	0.29	–
		Inhalation	0.19	0.12	–
		Dermal Contact	0.19	0.09	–
		Total (HI)	0.9	0.5	–
	As	Ingestion	0.45	0.25	1.1×10^{-4}
		Inhalation	0.16	0.08	1.1×10^{-4}
		Dermal Contact	0.14	0.07	1.1×10^{-4}
		Total (HI)	0.75	0.4	1.1×10^{-4}
Residential Zone	Pb	Ingestion	0.61	0.33	–
		Inhalation	0.22	0.14	–
		Dermal Contact	0.22	0.13	–
		Total (HI)	1.05	0.6	–
	As	Ingestion	0.51	0.26	1.2×10^{-4}
		Inhalation	0.19	0.1	1.2×10^{-4}
		Dermal Contact	0.15	0.09	1.2×10^{-4}
		Total (HI)	0.85	0.45	1.2×10^{-4}

risk levels of approximately 1.3×10^{-4}, marginally exceeding the U.S. EPA acceptable limit of 1×10^{-4}. While this marginal exceedance does not indicate immediate danger, it underscores potential long-term risks from sustained exposure and bioaccumulation. Considering As's strong associations with skin, lung, and bladder cancers, these findings highlight the importance of integrating carcinogenic risk factors into urban soil monitoring, public health initiatives, and risk management approaches (Table 6).

Ecological risk assessment

The ecological risk assessment of heavy metal contamination in urban soils revealed significant concerns, particularly in industrial and roadside zones, where PERI values were markedly elevated. Cd and Hg were the primary contributors, with PERI values of 212.7 and 174.3, and individual risk factors (Er_i) of 197.4 and 163.5, indicating moderate to high ecological risk. These values reflect intense anthropogenic pressures, including industrial emissions and vehicular exhaust. Cadmium negatively impacts soil microbial communities, lowers fertility, and can seep into groundwater. In contrast, Hg is neurotoxic and likely to biomagnify through food chains, creating risks to both humans and wildlife. The Geoaccumulation Index (Igeo) further highlighted contamination patterns, identifying Pb and Zn as major pollutants, with over 25% of sampled sites in industrial and roadside zones classified as moderately to heavily polluted. Elevated concentrations of Cr, Ni, and Co were observed in industrial zones, attributed to metal processing and industrial runoff, whereas roadside locations were characterized by Pb, Zn, and Cu, which are reflective of emissions from traffic. Hg and As exhibited a more diffuse

Table 7: Ecological risk assessment for heavy metal contamination in urban soils.

Zone	Metal	PERI Value	Er_i (Cd)	Er_i (Hg)	Igeo classification (Pb)	Igeo classification (Zn)
Industrial Zone	Cd	212.7	197.4	-	Moderately to heavily polluted	-
	Hg	174.3	-	163.5	-	-
Roadside Zone	Cd	188.9	176.8	-	Moderately polluted	-
	Hg	149.8	-	136.7	-	-
Recreational Zone	Cd	68.4	82.3	-	Low to moderate pollution	Low pollution
	Hg	58.6	-	71.1	-	-
Residential Zone	Cd	114.6	128.7	-	Low to moderate pollution	Low pollution
	Hg	101.2	-	119.8	-	-

distribution, indicating contributions from long-range atmospheric deposition and small-scale industry. The implications of these findings are evident for land management, cleanup strategies, and public governance. Areas with very high ecological risk should be prioritized for restricted or controlled land uses, avoiding residential, recreational, or agricultural development without prior remediation. Remediation strategies such as phytoremediation and the use of soil amendments, can help decrease metal bioavailability, and consistent soil monitoring is necessary to assess the effectiveness of these interventions. Stronger enforcement of industrial emission standards and traffic-related pollution controls, integrated with urban planning, will help prevent further contamination. This assessment establishes a framework for informed decision-making by connecting numerical risk indices to actionable management strategies, thereby safeguarding both ecosystem and public health in Astana (Table 7).

Impacts of heavy metal contamination on soil microbial activity

The MBC values indicate a clear gradient of declining soil microbial activity across different land-use types, reflecting the impact of heavy metal contamination. The highest MBC was recorded in peri-urban reference soils (312.7 ± 23.6 milligrams of carbon per kilogram of soil (mg C/kg)), suggesting healthy and active microbial communities in less-disturbed areas. Recreational areas maintained moderately high MBC levels (259.4 ± 19.1 mg C/kg), indicating relatively low anthropogenic influence. In contrast, residential soils exhibited reduced microbial biomass (187.9 ± 16.4 mg C/kg), likely due to increasing urban pressures. The lowest MBC values were observed in industrial (126.4 ± 12.3 mg C/kg) and roadside soils (109.2 ± 11.2 mg C/kg), coinciding with higher enrichment of Pb, Cd, and Hg. These findings reveal that elevated heavy metal levels greatly diminish microbial biomass, potentially jeopardizing soil health, nutrient cycling, and the overall functioning of ecosystems in highly urbanized regions (Fig. 5).

The results for basal soil respiration (BSR) and DHA indicate a significant adverse effect of heavy metal pollution on soil microbial activity across various land-use categories. Peri-urban reference soils exhibited the highest BSR (2.87 mg CO_2-C/kg/d) and DHA (3.12 µg TPF·g/h), indicating healthy microbial activity. Residential soils showed moderate reductions in BSR (1.96 mg CO_2-C/kg/d) and DHA (1.88 µg TPF·g/h), while industrial and roadside soils recorded the lowest BSR (~1.5 mg CO_2-C/kg/d) alongside severely suppressed DHA (~1.0 µg TPF·g/h). These results suggest that increased levels of heavy metals in urban areas significantly hinder microbial metabolism and enzyme function, which may lead to disruptions in soil fertility and nutrient cycling (Table 8).

The findings regarding heavy metal levels in urban soils highlight the considerable effect of human activities, particularly in regions affected by vehicle emissions, industrial waste, and atmospheric deposition. Elevated levels of Pb, Zn, Cu, Cr, Ni, and As were predominantly observed in roadside and industrial zones, indicating that urban soils act as reservoirs for these contaminants. This spatial variability reflects complex interactions between pollution sources and the urban environment. As noted by Duan *et al*. (2024), this heterogeneity is frequently influenced by the interactive effects of spatial drivers, with combinations of environmental variables providing more significant explanatory power regarding heavy metal distribution compared to isolated factors. Their integration of Geodetector,

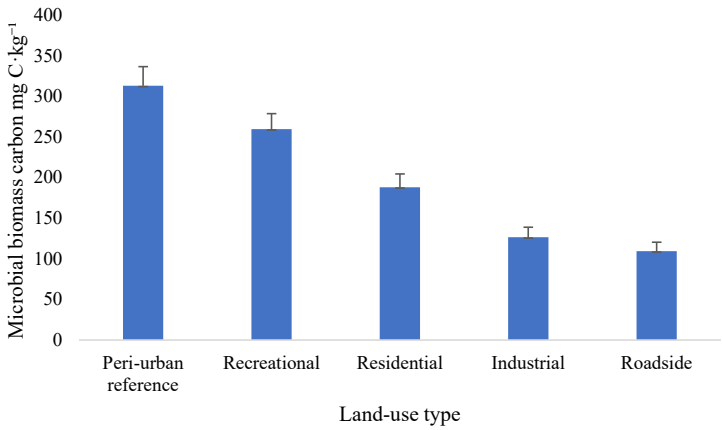

Fig. 5: Microbial biomass carbon by land-use

Table 8: Effects of heavy metal contamination on soil microbial activity across different land-use types (mean ± standard deviation)

Land-use type	Basal soil respiration (milligrams of carbon dioxide–carbon per kilogram of soil per day)	Dehydrogenase activity (micrograms of triphenyl formazan per gram of soil per hour)	Percentage reduction in basal soil respiration relative to reference
Peri-urban reference	2.87 ± 0.15	3.12 ± 0.22	0
Recreational	2.42 ± 0.13	2.81 ± 0.20	15.7
Residential	1.96 ± 0.12	1.88 ± 0.12	31.7
Industrial	1.51 ± 0.10	1.12 ± 0.11	47.4
Roadside	1.49 ± 0.09	0.91 ± 0.10	48.1

Categorical Boosting (CatBoost), and SHapley Additive exPlanations (SHAP) techniques highlighted that metal distributions, particularly for Hg, Cd, and Zn, were shaped by source–flow–sink interactions and that these interactions vary in influence across space. Similarly, Feng *et al.* (2024), reported in Cangxi County that spatial patterns of Pb, Zn, Cr, and Ni were closely interconnected, with higher levels connected to human activities, especially in regions marked by intense agricultural and traffic engagement. Their source apportionment via PMF further supported the significance of transportation (30.64%) and mixed agricultural traffic sources (65.2%) as key contributors. The current study's observations are supported by these findings, which indicate that traffic and industrial emissions are the main contributors to urban soil contamination, underscoring the importance of implementing spatially explicit monitoring systems and advanced modeling tools to analyze pollutant dynamics. The integration of such approaches can enhance our understanding of contaminant interactions and inform targeted urban soil pollution management strategies. The spatial distribution of heavy metals in urban soils, as determined through geostatistical and spatial analysis, reveals distinct contamination gradients that align closely with land-use types and the proximity to industrial activities or high-traffic zones. In regions characterized by high levels of industrial activity and vehicle emissions, elevated levels of elements like Cd, Pb, and Zn are regularly detected, highlighting the significant impact of human activities on soil quality. For instance, Wang *et al.* (2020), reported that in Jiangsu Province, China, heavy metals exhibited both zonal and clustered spatial distributions, with high levels concentrated in industrial parks and developed urban centers along the Yangtze River; patterns strongly correlated with the distribution of industrial enterprises. This spatial connection emphasizes the crucial influence of industrialization in forming contamination profiles. Similarly, Ma *et al.* (2023), demonstrated that at non-

ferrous metal smelting sites, factors such as the proximity to sintering workshops, raw material yards, and electrolyzers significantly influenced the horizontal distribution of heavy metals like As, Cd, and Hg. In the vertical dimension, physicochemical properties such as soil moisture, pH, and lithology also played important roles. These results suggest that spatial variability is influenced not just by emission sources but also by subsurface conditions that control the movement and retention of pollutants. The PCA served as a critical analytical tool in identifying the predominant sources of heavy metal contamination in urban soils, revealing three principal contributors: vehicular emissions, industrial discharges, and atmospheric deposition. The findings underscored the leading role of vehicular emissions in contributing to soil pollution, in agreement with prior research that emphasizes the substantial influence of traffic-related pollutants on both soil and air quality in urbanized regions. For instance, Ghose *et al.* (2004), documented that vehicular emissions in Kolkata exceeded permissible levels for key pollutants, severely degrading air quality and threatening public health. Similarly, Zhang and Batterman (2013), demonstrated that traffic congestion not only elevated nitrogen dioxide (NO_2) concentrations near roadways but also increased morbidity and mortality risks for exposed populations. The identification of industrial emissions as a secondary but substantial source further corroborates findings from urban and peri-urban industrial zones, where localized discharges contribute to heavy metal deposition (Sanad *et al.*, 2025). Industrial activities often emit metals such as Pb, Cd, and As, which accumulate in adjacent soils and present long-term ecological and human health risks (Angon *et al.*, 2024). Despite its smaller share of the variance, atmospheric deposition, which comes from the long-range transport of pollutants, has been identified as a notable contributor, highlighting the broader environmental implications of air pollution. The application of the Positive Matrix Factorization (PMF) model strengthened the results obtained from the PCA by providing a more detailed and quantitative apportionment of heavy metal sources in urban soils. Both models consistently identified traffic-related emissions, industrial discharges, and atmospheric deposition as the principal contributors to contamination, highlighting the robustness and complementarity of the multivariate techniques. Moreover, PMF identified traffic-related emissions as the leading contributor to the heavy metal burden, further supporting the expanding evidence that points to vehicles as a major source of urban pollutants. This aligns with recent studies, such as Tafidis *et al.* (2024), which demonstrated that fine particulate matter ($PM_{2.5}$) concentrations in Dublin were significantly influenced by urban traffic dynamics, with Gaussian Process Regression models identifying spatial proximity to intersections as a key predictor of pollutant levels. Furthermore, Reche *et al*. (2022), indicated that municipalities with inadequate non-motorized transport systems and poor public transport accessibility had higher levels of $PM_{2.5}$ and NO_2 from traffic, contributing to discernible health issues. The PMF model's strong correlation between observed and reconstructed heavy metal concentrations further validates its reliability for source attribution. These findings emphasize the need for targeted emission control strategies, particularly focusing on urban traffic management. As highlighted by Rautela and Goyal (2024), integrating advanced forecasting tools such as AI and machine learning can improve spatial-temporal pollution assessment and support the design of context-specific mitigation strategies. Consequently, thorough interventions, such as minimizing traffic emissions, managing industrial waste, and utilizing intelligent pollution monitoring technologies, could greatly alleviate soil and air contamination in city settings. Moreover, the study underscores substantial human health and ecological risks associated with heavy metal contamination in urban soils, particularly affecting children due to their higher soil ingestion rates and lower body mass. Consistent with findings from Shetty *et al.* (2024), elevated hazard index (HI) values for Pb and As in high-exposure areas, such as industrial and roadside zones, indicate significant non-carcinogenic and marginal carcinogenic risks, necessitating urgent public health interventions in sensitive locations like schoolyards and residential areas near major roads. From an ecological standpoint, increased concentrations of Cd and Hg were linked to moderate to high potential ecological risk index (PERI) values, supporting findings by Caković *et al*. (2021), which indicated that Cd surpassed allowable levels in all analyzed soils of protected natural reserves, designating extensive

regions as high ecological risk areas. Over 25% of sampled urban sites in the present study were categorized as "moderately to heavily polluted" by Pb and Zn, highlighting potential long-term degradation of soil functions and biodiversity. The integration of risk indices, land use data, and PMF source contributions in spatial analysis has identified contamination hotspots close to highways, industrial facilities, and densely populated urban regions. This geostatistical-spatial risk mapping approach aligns with methodologies employed in southern Italy by Ducci *et al.* (2017), who applied an integrated environmental characterization strategy to delineate risk zones across heterogeneous land uses. The attribution of these contamination patterns predominantly to anthropogenic sources; such as vehicular emissions and industrial discharges; is further supported by probabilistic receptor modeling and Monte Carlo simulations, as applied in the study by Alsafran *et al.* (2021), which found that consumption of leafy vegetables grown in polluted soils posed significant non-carcinogenic and carcinogenic risks due to elevated levels of As, Cr, and Ni.

CONCLUSION

This study delivers compelling evidence indicating that urban soils in rapidly evolving cities are profoundly affected by heavy metal contamination, with human-driven activities including vehicle exhaust, industrial functions, and urban building identified as the primary causes. The integration of advanced spatial mapping, source apportionment using PCA and PMF, and comprehensive ecological and human health risk assessments allowed for a detailed understanding of both the distribution patterns and the potential impacts of heavy metals across different land-use types. The results revealed notably elevated concentrations of toxic metals, including Pb, Cd, and Hg, especially in high-traffic and industrial zones, which pose substantial risks to human health, with children and other vulnerable populations being particularly susceptible, as well as to soil quality and broader ecosystem integrity. The recognized spatial inconsistency of contamination points out that risks are not evenly distributed in urban settings, stressing the vital importance of site-specific mitigation approaches. Areas characterized by mixed industrial and residential land use demonstrated the highest cumulative contamination indices, suggesting synergistic effects from multiple pollution sources that necessitate targeted monitoring and remediation. This study highlights the significance of merging geostatistical modeling with multivariate source identification and risk assessment frameworks, offering a solid, data-driven basis for managing urban environments. Such integration facilitates the prioritization of high-risk zones, optimizes the allocation of remediation resources, and supports informed decision-making in urban planning and environmental regulation. Furthermore, the study underscores the extensive applicability of these techniques to other swiftly urbanizing regions globally, presenting a transferable framework for the assessment, mapping, and management of urban soil contamination. The results highlight an urgent need for policy interventions, including stricter emission controls for vehicles and industries, improved industrial waste management, sustainable urban planning that considers soil quality preservation, and the adoption of soil remediation programs tailored to local contamination patterns. In parallel, fostering public awareness, encouraging community participation in pollution reduction initiatives, and promoting safe urban agricultural practices can significantly reduce human exposure to toxic metals. Prompt and sustained interventions, driven by scientific findings, are imperative to alleviate risks, defend public health, conserve ecosystem services, and secure the lasting sustainability of urban landscapes in response to fast-paced urbanization and industrial development. Feasible remediation strategies include phytoremediation using metal-accumulating plants, soil amendments to immobilize bioavailable metals, and restriction of sensitive land uses in identified hotspots. Economic feasibility is favorable given low-cost phytoremediation options and urban green space integration. Sustainable urban planning, involving emission controls, zoning regulations, and persistent monitoring, plays a vital role in alleviating additional contamination. Scenario analysis indicates that without interventions, projected urban expansion and industrial growth will exacerbate contamination hotspots, increase human exposure, and compromise soil ecosystem services.

AUTHOR CONTRIBUTIONS

A. Zandybay conceptualized the study, designed

the sampling framework, and coordinated field data collection. A. Kydyrova performed laboratory analyses, including heavy metal digestion and ICP-MS measurements, and assisted in data validation. A. Karilkhan conducted spatial analysis, developed geostatistical models, and supported interpretation of results. S. Gulnur contributed to statistical modeling, including PCA, HCA, and PMF analyses, and assisted in figure preparation. A. Daribay participated in ecological and human health risk assessments and helped draft sections of the results. T. Mkilima, the corresponding author, supervised the study, guided data interpretation, critically revised the manuscript, and finalized it for submission.

ACKNOWLEDGEMENT

This study was carried out with the financial support of grant funding for scientific and (or) scientific and technical projects for 2023–2025 from the Ministry of Science and Higher Education of the Republic of Kazakhstan [IRN AP19679898].

CONFLICT OF INTEREST

The authors declare that there is no conflict of interests regarding the publication of this manuscript. In addition, the ethical issues, including plagiarism, informed consent, misconduct, data fabrication and/or falsification, double publication and/or submission, and redundancy have been completely observed by the authors.

OPEN ACCESS

©2025 The author(s). This article is licensed under a Creative Commons Attribution 4.0 International License, which permits use, sharing, adaptation, distribution and reproduction in any medium or format, as long as you give appropriate credit to the original author(s) and the source, provide a link to the Creative Commons license, and indicate if changes were made. The images or other third-party material in this article are included in the article's Creative Commons license, unless indicated otherwise in a credit line to the material. If material is not included in the article's Creative Commons license and your intended use is not permitted by statutory regulation or exceeds the permitted use, you will need to obtain permission directly from the copyright holder. To view a copy of this license, visit: http://creativecommons.org/licenses/by/4.0/

PUBLISHER'S NOTE

GJESM Publisher remains neutral with regard to jurisdictional claims in published maps and institutional afflictions.

Negative AI Statement

The author(s) declare that no AI tools or services were not used or not highly applied during the preparation of this work.

ABBREVIATIONS

%	Percent
%CV	Percentage coefficient of variation
ADI	Average daily intake
ArcGIS	Aeronautical reconnaissance coverage geographic information system
As	Arsenic
B_n	Geochemical background concentration
CatBoost	Categorical Boosting
Cd	Cadmium
C_n	Measured concentration of metal in soil
cm	Centimeter
Co	Cobalt
Cr	Chromium
CR	Carcinogenic risk
CSF	Cancer slope factor
Cu	Copper
Er_i	Individual ecological risk factor
FW	Freshwater
g	Gram
GIS	Geographic information system
GPS	Global positioning system
GRSP	Glomalin-related soil proteins
g/m^2	Grams per square meter
HCA	Hierarchical cluster analysis
Hg	Mercury
HCl	Hydrochloric acid
HI	Hazard index
HNO_3	Nitric acid
HQ	Hazard quotient

IBM	International business machines
ICP-MS	Inductively coupled plasma mass spectrometry
Igeo	Geoaccumulation index
KMO	Kaiser-meyer-olkin
kg	Kilogram
L	Liter
log_2	Base-2 logarithm
m	Meter
mg	Milligram
mg/kg	Milligram per kilogram
Mn	Manganese
mL	Milliliter
MΩ·cm	Megaohm-centimeter
n	Sample size indicator
Ni	Nickel
NIST	National Institute of Standards and Technology
NO_2	Nitrogen dioxide
PCA	Principal component analysis
Pb	Lead
PERI	Potential ecological risk index
pH	Potential of hydrogen
PLI	Pollution load index
PM	Particulate matter
PM2.5	Particulate matter ≤ 2.5 micrometers
PM10	Particulate Matter ≤ 10 micrometers
PMF	Positive matrix factorization
RAGS	Risk assessment guidance for superfund
RSD	Relative standard deviation
RMSE	Root mean square error
SHAP	SHapley Additive exPlanations
SPSS	Statistical package for the social sciences
SRM	Standard reference material
USA	United States of America
USEPA	United States Environmental Protection Agency
v/v	Volume per volume
Zn	Zinc

REFERENCES

Idroes, G.M.; Rezeki, D.P.; Khairi, K.; Khairan, K.; Idroes, R.; Suhartono, E.; Prasetio, R.; Rahman S.A.; Suhendrayatna, S., (2024). Validation of heavy metals in geothermal to support water management practices and mitigation strategies. Global J. Environ. Sci. Manage., 10(SI): 153-166 **(14 pages).**

Ali, H.; Khan, E.; Ilahi, I., (2019). Environmental chemistry and ecotoxicology of hazardous heavy metals: environmental persistence, toxicity, and bioaccumulation. J. Chem., 1–14 **(14 pages)**.

Alsafran, M.; Usman, K.; Rizwan, M.; Ahmed, T.; Al Jabri, H., (2021). The carcinogenic and non-carcinogenic health risks of metal(oid)s bioaccumulation in leafy vegetables: A Consumption Advisory. Front. Environ. Sci., 9: 742269 **(10 pages)**.

Amodio, M.; Catino, S.; Dambruoso, P.R.; De Gennaro, G.; Di Gilio, A.; Giungato, P.; Laiola, E.; Marzocca, A.; Mazzone, A.; Sardaro, A.; Tutino, M., (2014). Atmospheric deposition: Sampling procedures, analytical methods, and main recent findings from the scientific literature. Adv. Meteorol., 161730 **(12 pages).**

Angon, P.B.; Islam, M.S.; KC, S.; Das, A.; Anjum, N.; Poudel, A.; Suchi, S.A., (2024). Sources, effects and present perspectives of heavy metals contamination: Soil, plants and human food chain. Heliyon. 10: e28357 **(16 pages)**.

Bettinelli, M.; Beone, G.M.; Spezia, S.; Baffi, C., (2000). Determination of heavy metals in soils and sediments by microwave-assisted digestion and inductively coupled plasma optical emission spectrometry analysis. Anal. Chim. Acta, 424: 289-296 **(8 pages)**.

Caković, M.; Beloica, J.; Simić, S.B.; Miljković, P.; Lukić, S.; Baumgertel, A.; Schwaiger, F., (2021). Diffuse pollution and ecological risk assessment in ludaš lake special nature reserve and palić nature park (Pannonian basin). Forests. 12: 1461 **(19 pages)**.

Chen, L.; Wang, G.; Wu, S.; Xia, Z.; Cui, Z.; Wang, C.; Zhou, S., (2019). Heavy metals in agricultural soils of the Lihe River Watershed, East China: Spatial distribution, ecological risk, and pollution source. Int. J. Environ. Res. Public Health, 16: 22094 **(19 pages).**

Custodio, M.; Fow, A.; Chanamé, F.; Orellana-Mendoza, E.; Peñaloza, R.; Alvarado, J. C.; Cano, D.; Pizarro, S., (2021). Ecological risk due to heavy metal contamination in sediment and water of natural wetlands with tourist influence in the central region of Peru. Water, 13: 2256 **(16 pages).**

Das, S.; Sultana, K.W.; Ndhlala, A.R.; Mondal, M.; Chandra, I., (2023). Heavy metal pollution in the environment and its impact on health: Exploring green technology for remediation. Environ. Health Insights, 17: 11786302231168152 **(16 pages)**.

Ducci, D.; Albanese, S.; Boccia, L.; Celentano, E.; Cervelli, E.; Corniello, A.; Crispo, A.; De Vivo, B.; Iodice, P.; Langella, C.; Lima, A.; Manno, M.; Palladino, M.; Pindozzi, S.; Rigillo, M.; Romano, N.; Sellerino, M.; Senatore, A.; Speranza, G.; Fiorentino, N.; Fagnano, M., (2017). An Integrated Approach for the Environmental Characterization of a Wide Potentially Contaminated Area in Southern Italy. Int. J. Environ. Res. Public Health. 14: 693 **(27 pages)**.

Duan, D.; Wang, P.; Rao, X.; Zhong, J.; Xiao, M.; Huang, F.; Xiao, R., (2024). Identifying interactive effects of spatial drivers in soil heavy metal pollutants using interpretable machine learning models. Sci. Total Environ., 934: 173284 **(12 pages)**.

Feng, Z.; Chen, W.; Meng, Y.; Lu, H.; Shi, X.; Zhang, J., (2024). Spatial variability and source analysis of soil heavy metals: A case study of the key planting area of special agricultural products in Cangxi County, China. PLoS One, 19: e0303387 **(15 pages).**

Ghose, M.K.; Paul, R.; Banerjee, S.K., (2004). Assessment of the impacts of vehicular emissions on urban air quality and its management in Indian context: The case of Kolkata (Calcutta). Environ. Sci. Policy **(12 pages)**.

Hawrami, K.M.; Baset, A.K., (2024). Trace element concentrations, multivariate analysis and health risk potential of soils from urban and peri-urban agriculture. Global J. Environ. Sci. Manage., 10(4): 2045-2066 **(22 pages).**

Jaishankar, M.; Tseten, T.; Anbalagan, N.; Mathew, B.B.; Beeregowda, K.N., (2014). Toxicity, mechanism and health effects of some heavy metals. Interdiscip. Toxicol., 7(2): 60–72 **(13 pages)**.

Kuklová, M.; Kukla, J.; Hniličková, H.; Hnilička, F.; Pivková, I., (2022). Impact of Car Traffic on Metal Accumulation in Soils and Plants Growing Close to a Motorway (Eastern Slovakia). Toxics. 10: 183 **(12 pages)**.

Luo, S.; Chen, R.; Han, J.; Zhang, W.; Petropoulos, E.; Liu, Y.; Feng, Y., (2024). Urban green space area mitigates the accumulation of heavy metals in urban soils. Chemosphere, 350: 141266 **(14 pages)**.

Ma, Y.; Li, Y.; Fang, T.; He, Y.; Wang, J.; Liu, X.; Wang, Z.; Guo, G., (2023). Analysis of driving factors of spatial distribution of heavy metals in soil of non-ferrous metal smelting sites: Screening the geodetector calculation results combined with correlation analysis. J. Hazard. Mater., 445: 130614 **(15 pages)**.

Manzueta, R.; Kumar, P.; Ariño, A.H.; Martín-Gómez, C., (2024). Strategies to reduce air pollution emissions from urban residential buildings. Sci. Total Environ., 951: 175809 **(12 pages)**.

Mitra, S.; Chakraborty, A.J.; Tareq, A.M.; Bin Emran, T.; Nainu, F.; Khusro, A.; Idris, A.M.; Khandaker, M.U.; Osman, H.; Alhumaydhi, F.A.; Simal-Gandara, J., (2022). Impact of heavy metals on the environment and human health: Novel therapeutic insights to counter the toxicity. J. King Saud Univ. - Sci., 34: 101865 **(13 pages)**.

Nyiramigisha, P.; Komariah; Sajidan, (2021). Harmful Impacts of Heavy Metal Contamination in the Soil and Crops Grown Around Dumpsites. Rev. Agric. Sci., 9: 271–282 **(12 pages).**

Peter, L.L.; Yang, Y., (2019). Urban planning historical review of master plans and the way towards a sustainable city: Dar es Salaam, Tanzania. Front. Archit. Res., 8: 359–377 **(19 pages)**.

Perković, S.; Paul, C.; Vasić, F.; Helming, K., (2022). Human health and soil health risks from heavy metals, micro(nano) plastics, and antibiotic resistant bacteria in agricultural soils. Agronomy 12(12): 2945 **(18 pages)**.

Phaenark, C.; Phankamolsil, Y.; Sawangproh, W., (2024). Ecological and health implications of heavy metal bioaccumulation in Thai Fauna: A systematic review. Ecotoxicol. Environ. Saf., 285: 117086 **(26 pages)**.

Proshad, R.; Abedin Asha, S.M.A.; Abedin, M.A.; Chen, G.; Li, Z.; Zhang, S.; Tan, R.; Lu, Y.; Zhang, X.; Zhao, Z., (2024). Pollution area identification, receptor model-oriented sources and probabilistic health hazards to prioritize control measures for heavy metal management in soil. J. Environ. Manage., 369: 122322 **(18 pages)**.

Rana, M.S.; Wang, Q.; Wang, W.; Enyoh, C.E.; Islam, M.R.; Isobe, Y.; Kabir, M.H., (2024). Sources, Distribution, and Health Implications of Heavy Metals in Street Dust across Industrial, Capital City, and Peri-Urban Areas of Bangladesh. Atmosphere (Basel), 15: 1088 **(15 pages)**.

Rautela, K.S.; Goyal, M.K., (2024). Transforming air pollution management in India with AI and machine learning technologies. Sci. Rep., 14: 20412 **(15 pages)**.

Reche, C.; Tobias, A.; Viana, M., (2022). Vehicular Traffic in Urban Areas: Health Burden and Influence of Sustainable Urban Planning and Mobility. Atmosphere (Basel), 13: 598 **(14 pages)**.

Sanad, H.; Moussadek, R.; Mouhir, L.; Lhaj, M.O.; Dakak, H.; Zouahri, A., (2025). Geospatial analysis of trace metal pollution and ecological risks in river sediments from agrochemical sources in Morocco's Sebou basin. Sci. Rep., 15: 16701 **(16 pages)**.

Sánchez-Castro, I.; Molina, L.; Prieto-Fernández, M.-Á.; Segura, A., (2023). Past, present and future trends in the remediation of heavy-metal contaminated soil - Remediation techniques applied in real soil-contamination events. Heliyon. 9: e16692 **(15 pages)**.

Shetty, B.R.; Pai, B.J.; Salmataj, S.A.; Naik, N., (2024). Assessment of Carcinogenic and non-carcinogenic risk indices of heavy metal exposure in different age groups using Monte Carlo Simulation Approach. Sci. Rep., 14: 30319 **(16 pages)**.

Tafidis, P.; Gholamnia, M.; Sajadi, P.; Vijayakrishnan, S.K.; Pilla, F., (2024). Evaluating the impact of urban traffic patterns on air pollution emissions in Dublin: a regression model using google project air view data and traffic data. Eur. Transp. Res. Rev., 16: 47 **(12 pages)**.

Wang, Y.; Duan, X.; Wang, L., (2020). Spatial distribution and source analysis of heavy metals in soils influenced by industrial enterprise distribution: Case study in Jiangsu Province. Sci. Total Environ., 710: 134953 **(14 pages)**.

Yang, T.; Wu, F.; Luo, M.; Xiong, J.; Nie, X.; Cao, F.; Ruan, Y.; Li, F.; Huang, W.; Liang, T.; Yang, Y., (2024). Accumulation Pattern and Potential Ecological Risk of Heavy Metals in Topsoil as Affected by Diverse Sources in Different Ecosystems in Western Dabie Mountain. Forests. 15: 1116 **(16 pages)**.

Yang, Z.; Lu, W.; Long, Y.; Bao, X.; Yang, Q., (2011). Assessment of heavy metals contamination in urban topsoil from Changchun City, China. J. Geochemical Explor., 110: 221–229 **(9 pages).**

Zhang, K.; Batterman, S., (2013). Air pollution and health risks due to vehicle traffic. Sci. Total Environ., 444: 1–12 **(12 pages)**.

AUTHOR (S) BIOSKETCHES

Zandybay , A., Ph.D., Associate Professor, L.N. Gumilyov Eurasian National University, Astana, Kazakhstan.
- Email: *zandybay_a@enu.kz*
- ORCID: 0000-0001-8485-2988
- Web of Science ResearcherID: NA
- Scopus Author ID: 57340597900
- Homepage: https://fns.enu.kz/en/page/departments/department-of-environmental-management-and-engineering/professorial-and-teaching-staff

Kydyrova, A., MSc., Researcher, L.N. Gumilyov Eurasian National University, Astana, Kazakhstan.
- Email: *kmaraloishina@gmail.com*
- ORCID: 0000-0001-9682-3703
- Web of Science ResearcherID: NA
- Scopus Author ID: 59400858100
- Homepage: https://bulchmed.enu.kz/index.php/bulchmed/article/download/564/361

Karilkhan, A., MSc., Researcher, Abylkas Saginov Karaganda Technical University, Karagandy, Kazakhstan.
- Email: *ymbatoibakova@gmail.com*
- ORCID: 0000-0002-1568-7904
- Web of Science ResearcherID: NA
- Scopus Author ID: NA
- Homepage: http://fsd.unsyiah.ac.id/muksinumar/

Saspugaeva, G., Ph.D., Associate Professor, L.N. Gumilyov Eurasian National University, Astana, Kazakhstan.
- Email: *saspugayeva_gye@enu.kz*
- ORCID: 0000-0003-3223-3602
- Web of Science ResearcherID: NA
- Scopus Author ID: 57197720988
- Homepage: https://enu.kz/en/portfolio/2ae3294b4e58f7458e06e96f076423b9082fb99d3ece

Daribay , A., Ph.D., Professor, L.N. Gumilyov Eurasian National University, Astana, Kazakhstan.
- Email: *daribai_ao@enu.kz*
- ORCID: 0009-0008-3946-0684
- Web of Science ResearcherID: NA
- Scopus Author ID: 52663184800
- Homepage: https://fns.enu.kz/en/page/departments/department-of-environmental-management-and-engineering/professorial-and-teaching-staff

Mkilima, T., Ph.D., Lecturer, Department of Environmental Engineering and Management, The University of Dodoma, 1 Benjamin Mkapa Road, 41218 Iyumbu, Dodoma, Tanzania
- Email: *tmkilima@gmail.com*
- ORCID: 0000-0003-1170-0494
- Web of Science ResearcherID: AAQ-3820-2020
- Scopus Author ID: 57217095406
- Homepage: https://www.udom.ac.tz/staff/staff_profile?id=VDFSbk1RPT0=

HOW TO CITE THIS ARTICLE

Zandybay, A.; Kydyrova, A.; Karilkhan, A.; Saspugaeva, G.; Daribay, A.; Mkilima, T., (2025). Potential impact of urbanization on heavy metals accumulation in surface soils of rapidly urbanizing cities. Global J. Environ. Sci. Manage., 11(4): 1547-1566.

DOI: 10.22034/gjesm.2025.04.11

URL: https://www.gjesm.net/article_729218.html